A&A 469, 285–296 (2007)
DOI: 10.1051/0004-6361:20066911

Astronomy & Astrophysics

Absolute dimensions of eclipsing binaries⋆,⋆⋆

XXV. U Ophiuchi and the evolution and composition of 5 $M_\odot$ stars

L. P. R. Vaz[1], J. Andersen[2,3], and A. Claret[4]

[1] Departamento de Física, ICEX–UFMG, C.P. 702, BR-30.123-970 Belo Horizonte, MG, Brazil
e-mail: lpv@fisica.ufmg.br
[2] The Niels Bohr Institute, Astronomy, Juliane Maries Vej 30, 2100 Copenhagen, Denmark
e-mail: ja@astro.ku.dk
[3] Nordic Optical Telescope Scientific Association, Apartado 474, 38 700 Santa Cruz de La Palma, Spain
[4] Instituto de Astrofísica de Andalucía, CSIC, Apartado 3004, 18 080 Granada, Spain
e-mail: claret@iaa.es

Received 11 December 2006 / Accepted 29 March 2007

ABSTRACT

Context. Precise stellar masses and radii provide unique information on stellar evolution. In a Galactic context, they may also provide information on the evolution of the Solar neighbourhood.
Aims. We aim to determine absolute dimensions for the mid B-type eclipsing binary U Ophiuchi and compare the inferred ages and chemical compositions to those of other binary stars with masses near 5 $M_\odot$.
Methods. We determine masses, radii, $\log g$, $\log T_{\rm eff}$, and luminosities for the stars in U Oph from new radial velocities and *uvby* light curves. By improving the Wilson-Devinney code, we also derive precise apsidal-motion and light-time orbits of this triple system, using 353 times of minimum over 120 years. Finally, we compare the data for U Oph and three similar systems with the predictions of stellar models.
Results. The stars in U Oph have masses of $5.27 \pm 0.09\,M_\odot$ and $4.74 \pm 0.07\,M_\odot$, radii of $3.48 \pm 0.02\,R_\odot$ and $3.11 \pm 0.03\,R_\odot$; we argue that systematic errors are negligible. The apsidal motion period is exceptionally short, $U \sim 21$ yr, while the light-time orbit has $P_3 \sim 38.4$ yr. The precise $\log g$ values for DI Her, U Oph, V760 Sco, and MU Cas, all within 10% of 5 $M_\odot$, place them successively from the ZAMS to the TAMS, at ages of $5-100 \times 10^6$ yr. Current stellar evolution models fit both stars in each system very well if the (otherwise unconstrained) metal abundance Z is adjusted in each case.
Conclusions. More accurate data and/or binary systems with larger mass ratios are needed to actually *test* stellar models near 5 $M_\odot$. The different Z values found for these young, nearby systems suggest that disk stars form with a range of metal abundances even today, but more data are needed to confirm this result.

Key words. stars: binaries: eclipsing – stars: fundamental parameters – stars: evolution – Galaxy: evolution

1. Introduction

Accurate empirical stellar masses, radii, and luminosities are valuable test data for stellar evolution models (Andersen 1991). With the precise masses and radii obtainable in favourable eclipsing binaries (1–2%), differences in age and chemical composition can be studied in a degree of detail that is possible with few other techniques. Such studies can, therefore, yield information not only on the stars themselves, but also on the star formation history near the Sun. The evolution of the Solar neighbourhood is typically studied from samples of long-lived F and G stars (see e.g. Nordström et al. 2004); here we present a contrasting view of the most recent past, based on accurate data for eclipsing binaries with masses near 5 $M_\odot$.

As part of this study we have redetermined the absolute dimensions of the double-lined mid-B type eclipsing binary U Ophiuchi (HD 156247, Sp. type B4 V, $P = 1\overset{\rm d}{.}677$). U Oph is in fact one of the brightest binaries in the sky; yet, its properties are still not known to modern standards. It has a small orbital eccentricity ($e = 0.003$), apsidal motion of exceptionally short period ($U \sim 21.2$ yr), and shows light-time effects from a distant third star (Panchatsaram 1981) with an orbital period of ∼39 yr (Kämper 1986). A distant visual companion (20.″7 from U Oph, ∼4500 AU minimum physical separation, $V \sim 13$) has no impact on the analysis and is not discussed here.

The most recent comprehensive study of U Oph is by Holmgren et al. (1991), who determined masses from new digital spectra, using cross-correlation techniques, and reanalysed the existing light curves. Their results were in fair agreement with those by Popper & Carlos (1970), but left a suspicion of systematic effects, and the available light curves had poor phase coverage or photometric "complications" of obscure origin. Later photometry and polarimetry (Eritsian et al. 1998) and times of minimum (Wolf et al. 2002) have not materially improved our knowledge of the properties of the stars in U Oph.

As few good mass and radius determinations exist for stars above ∼4 $M_\odot$, we decided to obtain new spectroscopic observations and *uvby* light curves of U Oph. Preliminary mass values

⋆ Based on observations collected at the European Southern Observatory, La Silla, Chile.
⋆⋆ Table 5 is only available in electronic form at the CDS via anonymous ftp to cdsarc.u-strasbg.fr (130.79.128.5) or via http://cdsweb.u-strasbg.fr/cgi-bin/qcat?J/A+A/469/285

Table 1. Spectral lines adopted for radial velocity measurements in U Oph.

λ (Å)	Id.	Comment	λ (Å)	Id.	Comment
3819.637	He I		4267.167	C II	
3867.556	He I		4481.228	Mg II	
4120.837	He I	A only	4713.241	He I	A only

were included in the review by Andersen (1991); here we present a full analysis of all the data available at this time.

2. Spectroscopic data

2.1. Observations

Our 34 spectra of U Oph were obtained in 1980–1986 on fine-grain, high-contrast IIIa-J plates with the ESO 1.5 m telescope and coudé spectrograph at La Silla, Chile, at dispersions of 20 and 12.4 Å mm^{-1} (plate codes F and G, respectively). Average exposure times were ∼10 min. Our observing and measuring procedures, as well as the zero-point and accuracy of radial-velocity observations with this instrument, are described by Andersen & Nordström (1983a,b).

The star eclipsed at primary eclipse (star A) has stronger and broader lines than those of the secondary, star B (see also Popper 1981, Fig. 5). The spectral type is ∼B4, with lines broadened by rotation. The interstellar Ca II H and K lines are weak, but measurable.

2.2. Radial velocities and spectroscopic orbits

In early-type double-lined binaries, radial velocities measured from lines with broad damping wings (i.e. H and diffuse He I lines) are prone to serious systematic errors (Andersen 1991). Unfortunately, the spectra of fast-rotating mid-B binaries offer few alternatives (strong metallic or sharp He I lines). Moreover, in U Oph the stellar Ca II K lines are too weak to measure, and Mg II λ 4481 blends with He I λ 4471 at maximum line separation. All potentially useful lines in the spectrum were therefore measured and analysed for consistency as described by Andersen (1975b).

In the choice of lines upon which to base the final radial velocities, freedom from systematic (blending) error was given priority over ease of measurement. Thus, the final list (Table 1) contains only few, fairly weak lines. Internal mean error estimates from the line-to-line dispersion on each plate, σ, is 5.2 km s^{-1} (star A) and 7.8 km s^{-1} (B). Better precision could now be achieved from high-S/N digital spectra, but we believe that the lines selected yield masses free of significant systematic error. The zero-point of the velocities is defined by the lines found to be reliable in B-type spectra by Andersen & Nordström (1983a).

Our final mean radial velocities for U Oph are listed in Table 2. Phases are computed from the ephemeris of Sect. 4.2 for the period of our observations:

$$\text{Min. I} = \text{HJD } 2\,442\,621.6212 + 1^{\text{d}}.6773458 \cdot E. \quad (1)$$

The mean radial velocity of the interstellar Ca II H and K lines is -17.8 ± 0.5 km s^{-1} with a standard deviation of 2.7 km s^{-1}, in excellent agreement with Popper & Carlos' (1970) value of -18.4 km s^{-1}.

Table 2. Mean radial velocities, internal errors, and residuals (km s^{-1}) for U Oph. n: number of lines measured; *: half weight.

	Plate No.	HJD −2 440 000	Phase	Star A Vel.	m.e.	n	Star B Vel.	m.e.	n	(O−C) A	(O−C) B
F	7107	4385.6389	0.6719	149.9	5.0	6	−200.1	10.2	4	−0.5	−11.5
F	7112	4385.6981	0.7072	164.8	3.6	6	−204.1	3.3	4	−0.5	1.2
F	7113	4385.7630	0.7459	167.1	4.6	6	−211.4	7.0	4	−4.7	1.2
F	7118	4385.8358	0.7893	177.6	4.4	6	−217.8	9.9	4	11.2	−11.4
F	7188	4391.6674	0.2660	−190.5	6.0	6	205.1	4.0	4	1.5	10.2
F	7200	4391.6928	0.2812	−182.9	6.0	6	196.0	18.4	3	6.5	4.0
F	7203	4391.7581	0.3201	−171.8	1.7	6	185.1	6.6	4	3.7	8.7
F	7204*	4391.7714	0.3280	−172.5	5.1	6	166.7	11.1	4	−1.1	−5.2
F	7310	4395.7557	0.7034	165.2	1.0	4	−205.1	4.4	2	1.1	−1.2
F	7311	4395.7619	0.7071	162.1	4.4	5	−196.6	6.6	3	−3.2	8.6
F	7320	4395.8578	0.7642	166.7	4.0	5	−231.1	10.2	3	−4.5	−19.3
F	7321	4395.8632	0.7675	152.6	4.1	6	−201.0	3.5	4	−18.2	10.4
F	7329	4396.7651	0.3052	−178.6	6.9	5	175.1	10.3	4	3.5	−8.7
F	7330	4396.7705	0.3084	−183.4	5.8	6	185.1	4.5	4	−2.6	2.8
F	7333	4396.8340	0.3462	−152.4	5.5	4	161.5	2.1	3	8.2	2.8
F	7446	4650.8950	0.8123	155.7	6.4	4	−203.4	11.6	4	−2.4	−6.2
F	7447	4650.9012	0.8160	174.3	7.5	3	−178.3	3.1	2	17.9	17.0
F	7506	4654.8533	0.1722	−174.6	5.9	4	172.2	4.4	3	−3.1	6.2
F	7507*	4654.8620	0.1773	−177.0	2.9	6	163.4	8.4	3	−2.8	−11.6
F	7509*	4654.8886	0.1932	−184.0	6.2	4	180.4	10.4	3	−2.6	−2.7
F	7510*	4654.8945	0.1967	−189.8	4.0	3	176.1	7.5	3	−7.0	−8.5
G	11698	4654.9028	0.2017	−178.2	5.6	6	175.2	6.7	3	8.4	−11.4
G	11699	4654.9116	0.2069	−190.0	3.1	6	176.8	3.6	4	−3.7	−11.7
F	7520	4655.8755	0.7816	166.6	6.0	6	−198.4	8.4	4	−1.7	10.2
F	7521	4655.8833	0.7862	163.8	5.3	6	−204.9	5.4	4	−3.4	2.5
F	8242	5772.9145	0.7378	168.1	5.1	4	−211.1	6.2	4	−3.3	0.9
F	8243	5772.9241	0.7435	164.4	7.8	5	−207.1	8.4	3	−7.3	5.4
F	8356	6127.8134	0.3214	−182.3	6.0	5	185.7	3.7	3	−7.5	10.0
F	8408	6132.8680	0.3349	−173.0	4.2	6	171.5	9.2	4	−5.4	3.9
F	8409	6132.8802	0.3421	−165.4	2.5	6	167.6	6.3	3	−2.2	5.0
F	8654	6574.7736	0.7901	174.5	2.9	6	−195.1	7.3	4	8.4	11.1
F	8655	6574.7923	0.8012	167.0	3.6	6	−205.2	10.7	4	4.5	−3.1
F	8659	6574.8493	0.8352	158.6	4.3	6	−205.9	9.5	4	12.2	−21.9
F	8660	6574.8704	0.8478	134.6	6.6	4	−171.1	4.3	4	−3.9	4.2

The small orbital eccentricity of U Oph ($e = 0.003$) can be safely ignored in solving the spectroscopic orbit, and circular orbital elements determined from the data in Table 2 are listed in Table 3. Solutions were made with all observations weighted equally (except a few plates of lower quality given half weight), as well as with weights proportional to $1/\sigma^2$. The resulting elements were not significantly different, and average values are adopted in Table 3 and used to compute the O−C values in Table 2 and the curves plotted in Fig. 1. Similarly, the γ-velocities from separate solutions for the two stars are slightly different, as could be expected when different sets of lines are used, but not significantly so.

The scatter of the data around the computed radial-velocity curves (Table 2) is somewhat larger than the estimated internal errors. This is likely due to a tendency to remove outliers from the mean of very few lines, and the residuals show no correlation with phase. Thus, we find no significant evidence for any intrinsic velocity variability. The errors of the orbital elements were, of course, computed from the real dispersion of the velocities.

Table 3 also compares our orbital elements with the earlier results. Those by Popper & Carlos (1970) agree with ours within the errors, while Holmgren et al. (1991) find masses that are ∼6% lower, a typical result from blended, diffuse He I lines (see Andersen 1975a). As we rejected those lines in our study for that very reason, we consider our determination of the masses in U Oph to be the most reliable currently available.

Table 3. Circular orbital elements for U Oph. σ is the standard deviation of a single observation.

Element:	This paper	Popper & Carlos	Holmgren et al.
K_A (km s^{-1})	182.7 ± 1.2	179.6 ± 1.9	182 ± 1
K_B (km s^{-1})	203.3 ± 1.6	201.8 ± 2.9	197 ± 1
γ (km s^{-1})	−9.5 ± 1.2	−12.0 ± 2.0	−7.4 ± 0.5
σ_A (km s^{-1})	6.5	—	5.4
σ_B (km s^{-1})	8.9	—	7.0
m_B/m_A	0.899 ± 0.009	0.89 ± 0.02	0.924 ± 0.007
$m_A \sin^3 i\,(M_\odot)$	5.26 ± 0.09	5.11 ± 0.16	4.92 ± 0.05
$m_B \sin^3 i\,(M_\odot)$	4.73 ± 0.07	4.55 ± 0.12	4.54 ± 0.05
$a \sin i\,(R_\odot)$	12.79 ± 0.07	12.55 ± 0.05	12.64 ± 0.11

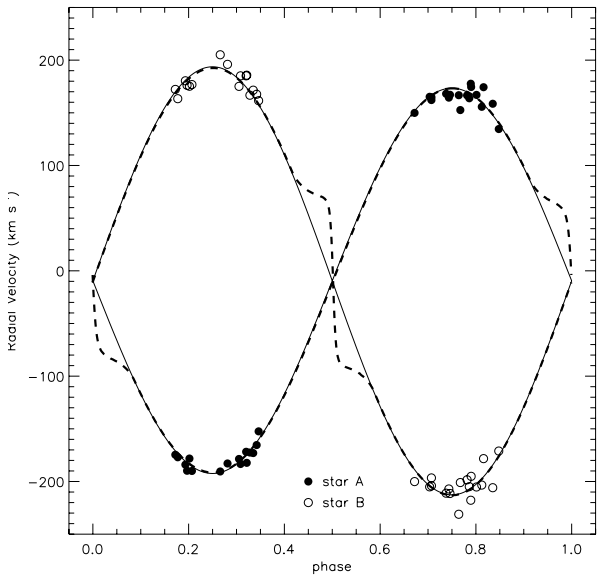

Fig. 1. Observed radial velocities and computed orbits for U Oph, for the circular solution of Table 3 (solid lines) as well as the eccentric solution of Sect. 5 (dashed). The only significant differences are due to eclipse effects, which are included in the WD model but do not affect the observed phases.

Our γ-velocity of U Oph agrees precisely with that predicted from the light-time orbit by Kämper (1986, Fig. 7); its variation during our observations is negligible.

2.3. Luminosity ratio and rotation

Interpolating the widths of unblended lines in U Oph among those in standard stars from Slettebak et al. (1975), we determine rotational velocities $(v \sin i)_A = 125 \pm 15$ km s^{-1} and $(v \sin i)_B = 95 \pm 15$ km s^{-1}. These values are in reasonable agreement with those by Koch et al. (1965): 107 ± 2 km s^{-1} (A) and 87 ± 18 km s^{-1} (B) and Holmgren et al. (1991): 125 ± 5 km s^{-1} (A) and 115 ± 5 km s^{-1} (B). Within the uncertainty of these results, they give no evidence for any deviation from synchronous rotation (Table 10), as expected for the derived age and parameters of the system.

A spectroscopic luminosity ratio was estimated from the equivalent widths of the Mg II λ4481 and He I λ4471 lines, taking into account the small difference in $T_{\rm eff}$ between the stars. The mean value is $W_B/W_A = 0.71 \pm 0.09$, in good agreement with the determination by Holmgren et al. (1991) and with the result from our light curve analysis (Table 10).

Table 4. Photometric data for U Oph (at phase $0^p.325$) and the comparison stars. Error estimates refer to the last digit given (all tables).

	U Oph	Comp. 1	Comp. 2	Comp. 3
HD	156247	154895	154445	156539
α_{2000}	$17^h16^m33^s$	$17^h08^m14^s$	$17^h05^m32^s$	$17^h18^m05^s$
δ_{1950}	+01°12′38″	−01°04′46″	−00°53′32″	+03°08′50″
Sp. type	B4 V	A1 V	B1 V	F2
V($0^p.325$)	5.872	6.061	5.615	6.867
	±2	±3	±3	±2
$b-y$	0.094	0.048	0.195	0.272
	±2	±1	±2	±3
m_1	0.045	0.149	0.000	0.139
	±2	±2	±1	±3
c_1	0.403	0.992	0.092	0.878
	±2	±3	±3	±7
β ($0^p.325$)	2.684	2.869	2.620	2.681
	±3	±2	±5	±1

Table 5. 645 *uvby* magnitude differences U Oph − HR 6367 in the instrumental system. Available only in electronic form at the CDS.

3. Photometric data

3.1. Observations

Using the six-channel photometer at the 0.5-m SAT telescope at ESO, La Silla, Chile (Nielsen et al. 1987), we observed U Oph in the Strömgren *uvby*Hβ system during 4 nights in 1992 (JA), 3 nights in 1993, and 18 nights in 1994 (LPRV). A circular diaphragm of 17″ diameter was used to exclude the visual companion. Three comparison stars, HR 6367, HR 6353 and SAO 122251, all within ∼3° of U Oph, were observed alternately with U Oph itself. General information on U Oph and the comparison stars is summarised in Table 4.

Extinction corrections and, if needed, linear or quadratic zero-point drift corrections were determined each night from all constant stars. All comparison stars were found to be constant throughout the three observing periods, and the observations of HR 6353 and SAO 122251 were transformed to those of HR 6367, using the mean magnitude differences computed over all nights. The standard deviation of a single magnitude difference between two comparison stars is $0^m.0048$ (Δu) and $0^m.0037$ (Δv, Δb and Δy).

Our *uvby* light curves of U Oph contain 645 points in each colour (114 from 1992, 203 from 1993 and 328 from 1994) and cover most phases at least twice. They are given in Table 5 and shown in Fig. 2.

Transformation equations and coefficients from the instrumental system of Table 5 to the standard system are given by Vaz et al. (1998; Table 2, Eqs. (1)–(4)). Following Olsen (1983), they have been determined from standard stars of spectral type F and earlier ($(b-y)_{\rm std} < 0.41$) and are valid for U Oph and all the comparison stars.

The nearby star HR 6412 (HD 165208) has often been used as a comparison for U Oph, e.g. by Koch & Koegler (1977) and Wolf et al. (2002). We observed it initially, but soon found it to undergo eclipses on 3 different nights, as discovered independently by the Hipparcos mission (HIP 84479). The star is now known as V2368 Oph (Kazarovets et al. 1999; but note that the period given in the Hipparcos and Tycho catalogues is incorrect). The variability of HR 6412 may well have been

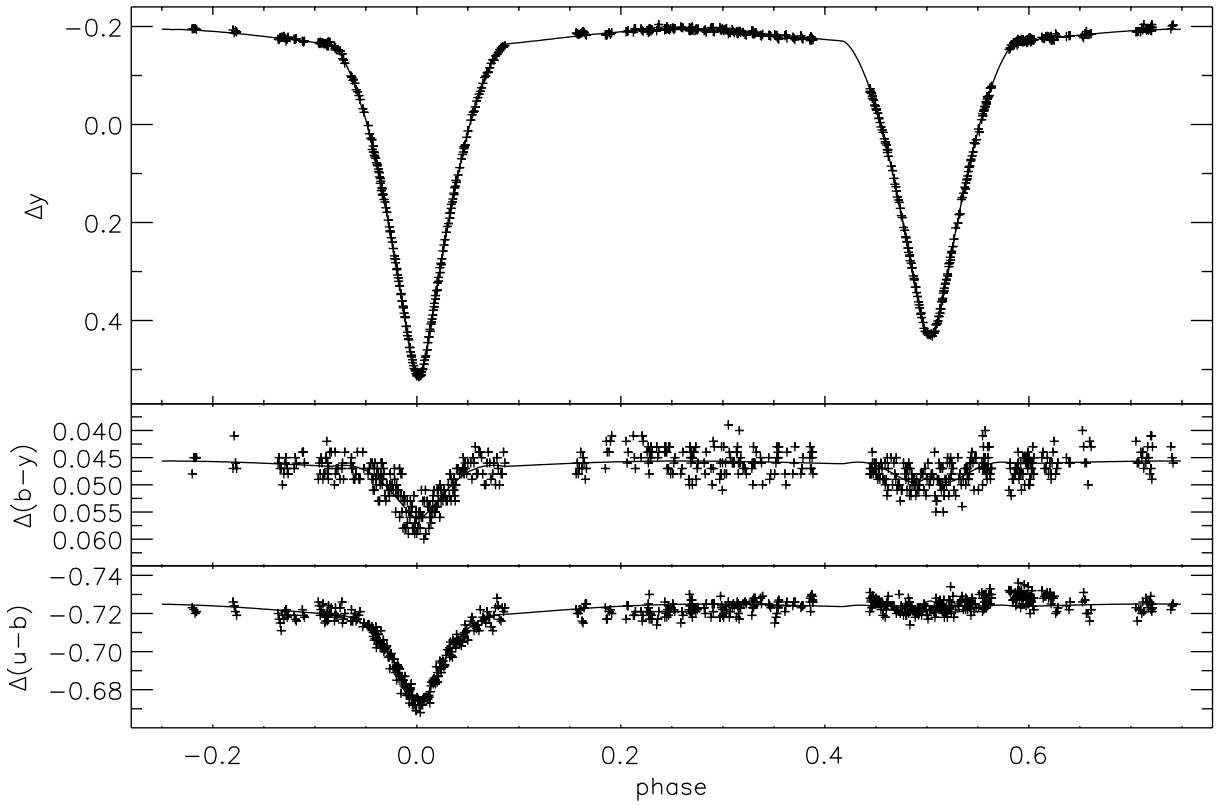

Fig. 2. y, $b-y$, and $u-b$ magnitude and colour differences between U Oph and HR 6367, in the instrumental system. The computed light curve corresponds to the final photometric solution (Sect. 5), for a mean periastron angle of 13°.6.

responsible for the unspecified photometric "complications" in U Oph reported in earlier literature. A complete analysis of V2368 Oph is in progress.

3.2. Interstellar reddening

Holmgren et al. (1991) found $E(b-y) = 0.158 \pm 0.005$ for U Oph, based on Crawford's (1979) calibration. Accepting Popper's (1980) $(b-y)_0$ (−0.072) for a spectral type of B5 together with Table 4 values, we find $E(b-y) = 0.166 \pm 0.003$. A third independent estimate can be made from our data (Table 9) and solution (L_3 and L_B/L_A, in each colour), using the theoretical $(b-y)_0$ for both components from Claret's (2004) models; this yields $E(b-y) = 0.171 \pm 0.004$. We adopt the average of these three values, $E(b-y) = 0.165 \pm 0.005$, corresponding to $A_V = 0.71 \pm 0.02$ ($A_V = 4.3\,E(b-y)$; Crawford 1978).

4. Apsidal-motion and light-time orbits of U Oph

4.1. Observed times of eclipse

Three new times of minimum were determined from our observations by the Kwee & van Woerden method (1956). They are listed in Table 6, with errors calculated from the agreement between the four colours.

Table 6 shows that eclipses now occur systematically earlier than predicted by the ephemeris of Kämper (1986, Eq. (10)), which included both the apsidal motion and the light-time orbit induced by the third star. Thus, the parameters of this ephemeris must be redetermined.

To do so on the best possible basis, we have searched the literature for all available eclipse timings for U Oph. In all, we found 512 individual times of minimum (334 pri, 178 s), determined with a wide range of techniques between 1882 and 2004. Many of the measurements are presented without error estimates, and a few are obvious mistakes (misprints or refer to another system). Eliminating redundant entries leaves us with 482 times (312 pri and 170 s), many referring to the same minimum (e.g. observed by different observers or by the same observer using different filters).

Table 6. New times of eclipse for U Oph. (O−C) values, cycle numbers, and phases refer to the ephemeris by Kämper (1986; Eq. (10)).

Year	HJD −2 440 000	Eclipse Type	(O−C) days	Cycle	Phase
1993	9155.737181 ±54	secondary	−0.0043	5169.5	0.49839 ±3
1993	9161.605377 ±72	primary	−0.0006	5173.0	0.99766 ±4
1994	9535.651549 ±77	primary	−0.0026	5396.0	0.99768 ±5

In the final analysis, we used the times of minimum from Table 6 (3 points) together with those listed by Kämper (1986, Tables I and II, 95 points), Wolf et al. (2002, 16 points), Klimec (1972, 1 point), Batten & Scarfe (1977, 3 points), Agerer & Hübscher (2003, 1 point), Diethelm (2004, 1 point), Zejda (2004, 1 point), Boskurt & Değirmenci (2005, 5 points), and 129 additional points selected from the "Eclipsing Binaries Minima Database"[1] of the *Supplemento ad Annuario Cracoviense*[2]. Two minima by Popovici (1971) show large residuals and were

[1] http://www.oa.uj.edu.pl/ktt/ktt.html
[2] http://www.oa.uj.edu.pl/ktt/rocznik/rcz_wstp.html

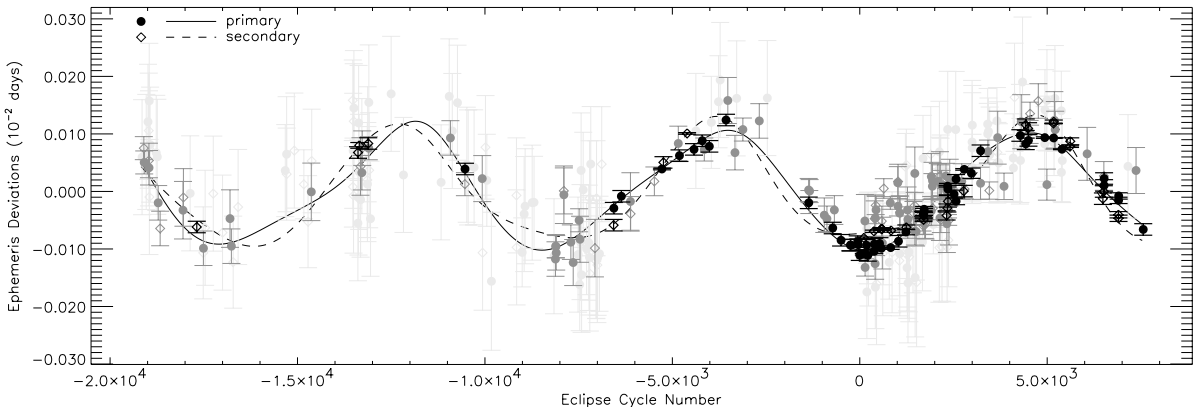

Fig. 3. O−C curve from a linear ephemeris for U Oph. The curves are computed for primary (solid line) and secondary minima (dashed) with the method by Lacy (1992), modified to include the light-time effect using the parameters of Table 7. Vertical bars show the errors of each point, used to weight the data during the optimisation. Points with errors >0$^{\rm d}$.005 are plotted in light grey (103 P, 55 S); points with errors between 0$^{\rm d}$.001 and 0$^{\rm d}$.005 (76 P, 39 S) in darker grey, and points with errors ≤0$^{\rm d}$.001 (50 P, 30 S) in black.

eliminated as probable mistakes (see also Panchatsaram 1981). Most of the points from Tables 10 and 11 of Plavec et al. (1960) were incorporated in our calculation, removing all visual determinations with residuals ≥0$^{\rm d}$.012 (we used 63 $T_{\rm pri}$ and 35 $T_{\rm sec}$). In total, 353 times of minimum (229 pri, 124 s) were used in the final analysis.

4.2. Computing orbital parameters

The ephemeris for eclipsing systems with apsidal motion is usually approximated by a series expansion (Giménez & Bastero 1995; Giménez & Garcia-Pelayo 1986). An exact method was proposed by Lacy (1992), based on a Levenberg-Marquardt optimisation technique (Press et al. 2000). For our work on U Oph, we have not only implemented Lacy's method in the Wilson-Devinney light-curve analysis code; we have also added the light-time effect, using the equations by Irwin (1952, 1959), which refer to the geometric centre of the orbit, not to the centre of mass of the system.

Modeling a time of eclipse amounts to computing the minimum projected separation between the centers of the eclipsing stars which, in turn, requires knowledge of the inclination of the eclipsing orbit. In order to distinguish the two sets of orbital elements in the following, P, i, e, and ω will refer to the eclipsing orbit, while P_3, i_3, e_3, and ω_3 will refer to the orbit of the third star. In practice, i is obtained from the light curve analysis which, in return, involves e and the current value of ω. Therefore the solution must be done iteratively, refining the ephemeris solution with the previous value of i, then iterating the light-curve solution (see Sect. 5) to refine the value of i and the other orbital elements with the improved ephemeris, etc.

The resulting orbital parameters are summarised in Table 7, and the fit to the data is shown in Fig. 3. According to this solution, the periastron angle of the eclipsing orbit varied from −4°.2 to 31°.4 during the photometric campaign, and from 152°.1 to 253°.8 while the spectroscopic observations were made.

The amplitude A of the light-time orbit is a measure of the projected semi-major orbital axis of the eclipsing pair around the centre of mass of the total system, $a_{12,3}$: $A = a_{12,3} \sin i_3/c$, where c is the speed of light. As for a single-lined spectroscopic binary, the mass function $f(\mathcal{M})$ of the triple system (also given in Table 7) can then be computed from $a_{12,3}$, i_3 and P_3:

$$f(\mathcal{M}) = \frac{(\mathcal{M}_3 \sin i_3)^3}{(\mathcal{M}_1 + \mathcal{M}_2 + \mathcal{M}_3)^2} = \frac{(a_{12,3} \sin i_3)^3}{P_3^2}. \quad (2)$$

Compared to the solutions by Kämper (1986) and Wolf et al. (2002), which are very similar, we find slightly, but significantly different periods for the apsidal motion and light-time orbit, both being about one year longer (and the anomalistic period correspondingly shorter). Our estimated (formal) errors are also much smaller, which we attribute to our more refined analysis and critical selection of observed times of minimum.

Figure 4 illustrates these differences and also shows when our observations were made. The effect of the extra motions on the phases in the eclipsing system was essentially constant while our photometry was done; hence, the phase of secondary minimum did not change significantly and we can treat the system

Table 7. Final elements of the apsidal motion and light-time orbits of U Oph (see text). U, $P_{\rm sid,ecl}$, and $P_{\rm ano,ecl}$ are the apsidal motion, sidereal, and anomalistic periods of the eclipsing system, respectively; $f(\mathcal{M})$ is the mass function of the third-star orbit. Standard deviations from the fits to primary, secondary, and all eclipses are given, weighting the observations as (obs. error)$^{-2}$. The unweighted standard deviation is 0$^{\rm d}$.0048 (6.9 min) in all cases, and the values of χ^2 are $\chi^2_{\rm all}$ = 609.6, $\chi^2_{\rm pri}$ = 406.5, and $\chi^2_{\rm sec}$ = 203.0 for 343, 219, and 114 degrees of freedom, respectively.

Apsidal Motion		Light-Time orbit	
parameter	final value	parameter	final value
$P_{\rm ano,ecl}$	1$^{\rm d}$.6777150	P_3 (year)	38.350
	±25		±79
e	0.003049	e_3	0.279
	±75		±13
ω_0, at T_0	−26°.926	ω_3	122°.2
	±38		±3°.0
ω_1 (°/cycle)	0.0791902	A (day)	0.010384
	±91		±57
T_0 (HJD)	2 440 484.68577	$T_{\rm periastron}$ (HJD)	2 435 169.
	±89		±112.
U (year)	20.88	$f(\mathcal{M})$	0.003951
	±14		±27
$P_{\rm sid,ecl}$	1$^{\rm d}$.677345899	$\sigma_{\rm pri}$ (229 points)	0$^{\rm d}$.00072
	±10		
$\sigma_{\rm all}$ (353 points)	0$^{\rm d}$.00062	$\sigma_{\rm sec}$ (124 points)	0$^{\rm d}$.00050

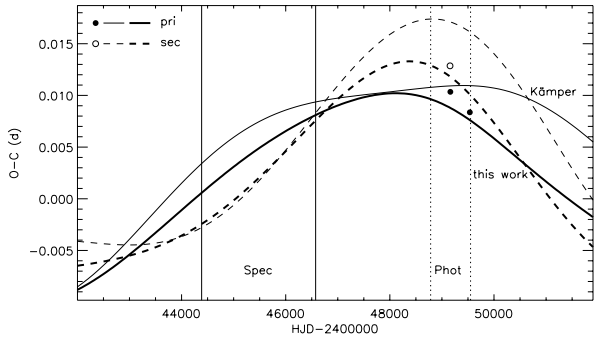

Fig. 4. O−C curves for primary (full) and secondary minima (dashed) from the linear ephemeris of Table 7 and from that by Kämper (1986, thin lines). Vertical solid and dotted lines mark the begining and the end of our spectroscopic and photometric observing periods, respectively, and our new minima are shown (the errors are smaller than the plotted symbols).

as if its orbit were static (see, e.g. Giménez & Clausen 1986). This is not true for the spectroscopic observations, however (see Fig. 4), so we decided to analyse the radial velocity and light curves simultaneously in the following.

5. Light-curve solutions

In order to analyse our light and radial-velocity curves of U Oph simultaneously, we have extensively improved our version of the WD model (Wilson & Devinney 1971; Wilson 1979, 1993, previously modified as described by Vaz et al. 1995 and Casey et al. 1998) so as to treat systems with significant apsidal motion (Vieira 2003) and/or light-time effects during the observing period.

Unfortunately, our light curves miss the first contact of secondary minimum. This might have made the determination of the eccentricity and periastron angle from the light curves alone uncertain, because the relative duration of the minima is poorly constrained. However, because we determine e as well as ω_0 and $\mathrm{d}\omega/\mathrm{d}t$ independently from the ephemeris analysis, this small gap does not affect the accuracy of our results.

5.1. Initial values

Initial values for the orbital inclination $i_{\rm ecl}$ and relative radii r_A, r_B were taken from Cester et al. (1978), initial ephemeris parameters from Kämper (1986, Table III). The mass ratio and axial rotations are from Sect. 2.2.

Effective temperatures are estimated from the *uvby* indices (Table 4), assuming $E(u-b)/E(b-y) = 1.60$ and $E(c_1)/E(b-y) = 0.24$ (Shobbrook 1976; Crawford 1974, 1975). The calibrations of Napiwotzki et al. (1993) and Davis & Shobbrook (1977, see also Moffat et al. 1983) then give near-identical values of $T_{\rm eff} = 16\,050 \pm 60$ K for the mean component of U Oph (errors derived from those of the photometry). The light-curve solutions and colour differences (see Fig. 2) indicate a temperature difference of 800 K between the two stars, so we adopted $T_{\rm eff,A} = 16\,440$ K in our light-curve solutions, very close to that given by Popper (1980) and Andersen (1991).

Reflection albedos and gravity brightening exponents were fixed at 1.0 for both components, as appropriate for stars with radiative envelopes (von Zeipel 1924; Eddington 1926; Milne 1927); see also Kopal (1968) and Eaton & Ward (1973). Linear limb-darkening coefficients were interpolated from the tables by Van Hamme (1993) for the current values of $\log g$ and $T_{\rm eff}$ (updated at every iteration). The radiative fluxes are described by atmosphere model tables (Kurucz 1979), updated from the original WD code (Vaz et al. 1995).

The mass function yields a plausible mass for the third component of ∼1 $M_\odot$. Assuming a Solar-like third star, we estimate initial values for the third light, L_3 of 0.0026, 0.0017, 0.0012, and 0.0009 in *ybvu*, respectively, in units of the light of the eclipsing system at quadrature ($L_3 = [\mathcal{L}_3/(\mathcal{L}_A + \mathcal{L}_B)]_{\rm quad}$).

Table 8. Standard deviations (in 10^{-5} mag) for the solution grid for U Oph (standard limb-darkening coefficients). (*) indicates that a negative value of L_3 was forced to zero.

$i_{\rm ecl}$	σ_u	σ_v	σ_b	σ_y
86.°5	*876	*690	*602	*558
87.°0	*692	*430	*388	407
87.°5	548	373	350	378
88.°0	553	350	333	363
88.°5	564	354	336	367
89.°0	570	365	346	380
89.°5	578	372	355	391
90.°0	581	381	363	397

5.2. Grid of solutions

The ephemeris parameters of Table 7 depend slightly on $i_{\rm ecl}$, so we generated a grid of solutions with $i_{\rm ecl}$ from 86.°5 to 90.°0 in steps of 0.°5. With the known orbital parameters ($i_{\rm ecl}$, e and ω, light-time amplitude) at each grid point and initial values from Sect. 5.1, we used the WD code to solve all four light curves simultaneously, leaving the stellar radii, the temperature of the secondary, the third light parameters, and a phase shift and internal luminosity scale for normalization as free parameters. Surface fluxes and limb-darkening coefficients were always kept consistent with the current values of $\log g$ and $T_{\rm eff}$.

For $i_{\rm ecl} \le 90°$, maximum values of L_3 are 0.034, 0.030, 0.027 and 0.022 in *ybvu*, respectively; on the other hand, for L_3 to remain non-negative requires $i_{\rm ecl} > 87°$.

In order to quantify the significance of any systematic differences between the computed and observed light as compared to random errors, we performed a formal R-statistic analysis of the O−C curves, (see e.g. Bruch 1999). For a given number n (645 here) and standard deviation σ of the observations, the R statistic allows to compute a probability, P_R, that random data with zero mean and standard deviation σ would have an even smaller value of R than computed from the actual residuals. P_R thus indicates the probability that no significant systematic trends remain in the residuals.

5.3. Fitting the u light curve

With standard limb darkening coefficients, the *vby* light curves all yield minimum σ and P_R for $88.°0 < i_{\rm ecl} < 88.°5$, and σ consistent with pure observational errors. However, in u the minimum occurs for $87.°5 < i_{\rm ecl} < 88.°0$ (Table 8), and σ_u is notably larger than the observational value.

In order to improve the fit in u, we had to increase the limb-darkening coefficients by 0.05 for both components, as done already for U Oph itself by Eaton & Ward (1973), Koch & Koegler (1977), and Holmgren et al. (1991), and for other OB binaries by Giménez et al. (1986) and Vaz et al. (1995, 1997, and references therein). All three (linear, linear-log and linear-square

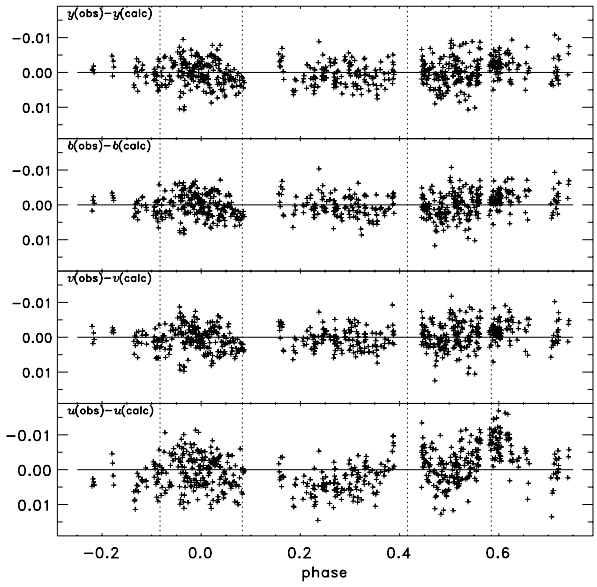

Fig. 5. *uvby* residuals from theoretical light curves for $i = 88\overset{\circ}{.}0$ and standard limb-darkening coefficients (Table 8). The dotted lines mark the beginning and end of the eclipses.

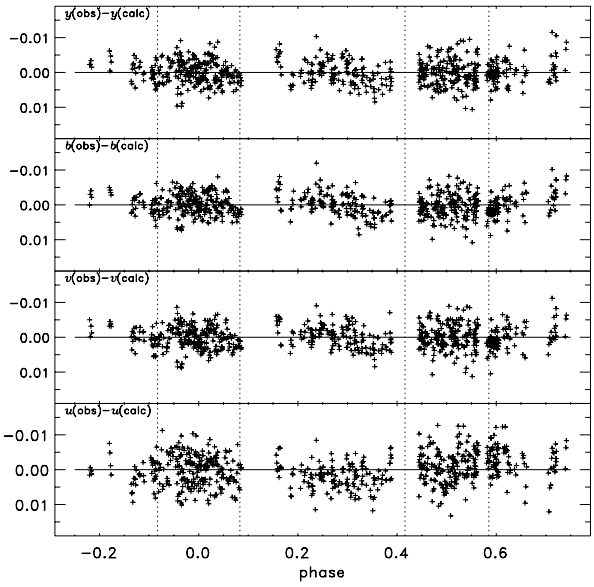

Fig. 6. *uvby* residuals from light curves computed with the adopted solution (Table 9); eclipses marked as in Fig. 5.

root) limb-darkening laws by Van Hamme (1993) were tested, but all gave a poor fit in *u*. The linear law gave a slightly better fit in the eclipses and was adopted.

Yet, even with this ad hoc correction to the limb-darkening coefficient in *u*, the fit to the *u* light curve was never as good as in *vby* (see Figs. 2, 5, and 6). σ_u was always larger than the observational error, and the values of P_R indicated that, in contrast to *vby*, significant systematic differences between the computed and observed *u* light curves remain.

These departures are readily seen in Fig. 5: the theoretical *u* light curve is always fainter than the observations near secondary minimum and brighter around quadratures (phases $0\overset{p}{.}25$ and $0\overset{p}{.}75$). After investigating all model parameters, we found that this discrepancy can be reduced by letting the WD code adjust also the gravity-brightening exponent, β, and reflection albedo, *w*, of the secondary component. The resulting β_B was close to the standard value for *convective* atmospheres, ∼0.43, while w_B increased to ∼1.3 (in contrast, both β_A and w_A remained very close to the theoretical values when left free to be adjusted, and were kept fixed in subsequent runs).

This is surprising, because at $T_B \sim 15\,500$ K the atmosphere of star B must be in radiative equilibrium, for which $\beta = w = 1$ as indeed they are in the just slightly hotter star A. Yet, modifying β_B and w_B as indicated reduces σ and P_R (i.e. the systematic trends) significantly, not only in *u* but also, if slightly, in *vby*.

The gravity-brightening exponents are dependent not only on the stellar atmosphere physics, but also on the internal stellar structure, since the distortions caused by rotation depend on it (Claret 2000). In particular, differential rotation might be a cause for β_B being <1, but it is intriguing that the otherwise very similar components of U Oph appear to be so different in this respect. One is also uncomfortable with a reflection albedo larger than unity.

It is, however, reassuring that despite these fairly radical steps, the radii of both stars and the effective temperature of the secondary change by less than 0.5% from the values obtained by keeping $\beta_B = w_B = 1$. Earlier theoretical studies, using stellar atmospheres, of monochromatic albedos (Vaz & Nordlund 1985; Nordlund & Vaz 1990), gravity-brightening exponents (Alencar & Vaz 1997), and the of effect of external irradiation on the gravity-brightening exponents (Alencar et al. 1999) and limb-darkening coefficients (Alencar & Vaz 1999) were performed for lower temperatures (≤7000 K), due to model limitations. The high quality of the present light curves suggests that these effects are real. It would be very important to extend these studies to higher temperatures, in order to check their reality in stars as hot as U Oph.

5.4. Final photometric solution

Starting with the previous solution for $i_{ecl} = 88\overset{\circ}{.}0$, the four light curves were solved simultaneously, but now including i_{ecl} as a free parameter together with r_A, r_B (through the gravitational pseudo equipotentials), T_B, β_B, and w_B. L_3 and normalization parameters in each colour were also included, allowing for the correlation between L_3 and i_{ecl}. The radial velocity curves were added to the fit, with the orbital semi-major axis and systemic velocity as additional free parameters. As before, limb-darkening coefficients (x^*) were kept consistent with the current *T* and $\log g$ values (x_u increased by 0.05 as in Sect. 5.3), and the orbital parameters of the third star (Table 7) were iterated with the ephemeris solution as well in order to maintain full internal consistency of all parameters.

In the solutions, we used both the traditional least-squares method built into the WD code and an implementation of the SIMPLEX method (Kallrath & Linnell 1987; Vieira 2003). Close to convergence, the former often oscillates around some value while the latter always homes in on the best parameter set, but alternating between the two methods was found very effective.

The parameters of the final solution are given in Tables 7 (apsidal motion and light-time orbit) and 9 (photometric elements) and shown in Figs. 1, 2, and 6. The derived radial-velocity amplitudes are $K_{A,ecc} = 182.4\,km\,s^{-1}$ and $K_{B,ecc} = 202.8\,km\,s^{-1}$, slightly lower than those of Table 3, but within the (same) errors.

As Fig. 1 shows, a circular orbit remains a very good approximation; moreover, the elements of Table 3 allow for a apparent differences in systemic velocity due to the different sets of lines and wavelengths used in the two stars. The *K* values from Table 3

Table 9. Final photometric elements for U Oph. r_A, r_B are in units of the orbital separation at periastron, and $r_{\rm volume}$ is the radius of a sphere with the same volume as the star; the errors given include those in M_B/M_A and Ω (the gravitational pseudo-potentials). Other errors are internal formal errors from the least-squares solution. Standard deviations of the unweighted residuals are given for both the light and radial-velocity curves.

Parameter	Value	Parameter	Value
$i_{\rm ecl}$ (°)	88.105 ±49	$r_{\rm A,pole}$	0.26631 ±70
$\Omega_{\rm A}$	4.6258 ±12	$r_{\rm A,point}$	0.2818 ±10
$\Omega_{\rm B}$	4.7921 ±14	$r_{\rm A,side}$	0.27128 ±78
$T_{\rm A}$ (K)	16 440.0 (fixed)	$r_{\rm A,back}$	0.27807 ±93
$T_{\rm B}$ (K)	15 587.8 ±4.7	$r_{\rm A,volume}$	0.27211 ±80
$L_{3,y}$	0.01884 ±28	$r_{\rm B,pole}$	0.2386 ±22
$L_{3,b}$	0.01500 ±27	$r_{\rm B,point}$	0.2500 ±25
$L_{3,v}$	0.01182 ±27	$r_{\rm B,side}$	0.2422 ±22
$L_{3,u}$	0.00206 ±21	$r_{\rm B,back}$	0.2475 ±24
a ($R_\odot$)	12.8111 ±76	$r_{\rm B,volume}$	0.2429 ±23
V_γ (km s^{-1})	−9.471 ±11	$q\left(\frac{M_{\rm B}}{M_{\rm A}}\right)$	0.89250 ±99
$\beta_{\rm A}$	1.0 (fixed)	$\beta_{\rm B}$	0.441 ±33
$w_{\rm A}$	1.0 (fixed)	$w_{\rm B}$	1.318 ±12
$x^*_{\rm bolo,A}$	0.711	$x^*_{\rm bolo,B}$	0.709
$x^*_{{\rm A},y}$	0.290	$x^*_{{\rm B},y}$	0.297
$x^*_{{\rm A},b}$	0.333	$x^*_{{\rm B},b}$	0.341
$x^*_{{\rm A},v}$	0.353	$x^*_{{\rm B},v}$	0.360
$x^*_{{\rm A},u}$	0.410	$x^*_{{\rm B},u}$	0.417
σ_y (mag)	0.00343	σ_b (mag)	0.00315
σ_v (mag)	0.00331	σ_u (mag)	0.00449
$\sigma_{\rm rv,A}$ (km s^{-1})	6.51	$\sigma_{\rm rv,B}$ (km s^{-1})	8.97

were therefore used to compute the absolute dimensions of the system.

The standard deviations from the final solution (Table 9) are just below the estimated observational errors of all four light curves (see also Fig. 6). Relative to the best solutions with standard, fixed $\beta_{\rm B}$ and $w_{\rm B}$ (and standard limb-darkening coefficients, Table 8), the improvement in σ_u is 17%, while σ_y, σ_b, and σ_v improve by 3%, 0%, and 0.6%, respectively. The P_R values for the adopted solution are 0.99, 0.95, 0.96, and 0.29 for the *uvby*, respectively, indicating that systematic deviations from the fits are insignificant.

6. Absolute dimensions of U Oph

Combining the result of Tables 3, 7, and 9 with the effective temperature derived in Sect. 5.1, we compute the absolute dimensions and other physical parameters of the eclipsing stars in U Oph listed in Table 10. Bolometric corrections from Popper (1980) and the currently preferred value of $M_{\rm bol,\odot} = 4.75$ were adopted.

The new masses and radii for U Oph are slightly, but significantly larger than the most recent determination by Holmgren et al. (1991). Given our improved data and more detailed analysis (see also Sect. 2.2), our results should be the most reliable currently available for U Oph. They agree within the errors with those listed by Andersen (1991), which were based on a preliminary analysis of the spectroscopic data included here.

Table 10. Physical parameters for U Oph.

	A (Primary)	B (Secondary)
Absolute dimension:		
Mass ($M_\odot$)	5.273 ± 0.091	4.738 ± 0.072
log M	0.7220 ± 0.0084	0.6756 ± 0.0066
Radius ($R_\odot$)	3.483 ± 0.020	3.109 ± 0.034
log R	0.5419 ± 0.0025	0.4927 ± 0.0047
log g (c.g.s.)	4.0682 ± 0.0098	4.128 ± 0.012
$V_{\rm synchr}$ (km s^{-1})	108.7 ± 0.6	96.6 ± 1.0
$\omega/\omega_{\rm orb}$	1.16 ± 0.14	0.99 ± 0.16
Photometric data:		
log $T_{\rm e}$(K)	4.2159 ± 0.0066	4.1928 ± 0.0070
log $L/L_\odot$	2.900 ± 0.027	2.709 ± 0.029
$M_{\rm bol}$	−2.499 ± 0.067	−2.022 ± 0.073
$M_{\rm V}$	−0.913 ± 0.067	−0.566 ± 0.073
$L_{\rm B}/L_{\rm A}$	0.727 ± 0.092	
Distance (pc)	216 ± 5	

6.1. Distance

The Hipparcos parallax of U Oph is (5.38 ± 0.83) mas, corresponding to a distance of 186^{+34}_{-25} pc. The distance given in Table 10 is based on the absolute radii, adopted effective temperatures, bolometric corrections (Popper 1980), third light (Table 9), calibrated visual magnitude (Table 4) and interstellar extinction, $A_{\rm V} = 0.71 \pm 0.02$ (Sect. 3.2). The corresponding parallax, (4.63 ± 0.11) mas, agrees with the Hipparcos result within the errors. The solution quality field (H61) in the Hipparcos Catalogue is flagged "S" (suspected non-single), which may explain the relatively large error of the Hipparcos parallax.

6.2. The third star

The mass function of the light-time orbit (Eq. (2), Table 7) can be used to estimate the mass of the third star in U Oph. Table 11 presents results for a range of possible values of i_3.

The final amounts of third light (Table 9) are not far from our initial guess (end of Sect. 5.1), but have a different colour dependence, being smaller at y, b and slightly larger in u. Combining our photometric data, final solution and physical parameters (Tables 4, 9 and 10) with the WD monochromatic solutions for b and y, we find $(b-y)_{L_3,0} = 0.338 \pm 0.009$, corresponding to a main-sequence star of spectral type ~F7 (Popper 1980). Assuming a black-body spectrum and using the colours and radii of the Claret models (2004), $L_{3,uvby}$ can be reasonably well reproduced if the third star is a (non-eclipsing) binary containing identical stars of $M = 1.48\,M_\odot$ at the same age as U Oph, 4×10^7 yr (thus with $R = 1.45\,R_\odot$, $T_{\rm eff} = 7000$ K). Both estimates are consistent and in reasonably good agreement despite the non-standard parameters of the u light curve (Sect. 5.3), which may affect the value of L_{3u}. If the total mass of the third body is $3.0\,M_\odot$, the third-body orbit should have $i_3 = 16\overset{\circ}{.}76 \pm 0\overset{\circ}{.}08$, and $a_{12,3}$ (Table 7) then leads to $a_{12,3} = (6.230 \pm 0.036)$ AU.

U Oph would then appear to be a hierarchical (i.e. triple, possibly quadruple) system with non-coplanar orbits, the larger of which has a semi-major axis projected on the sky of up to 28 mas

Table 11. Estimate of the mass of the third body by using Eq. (2) and Table 7 for different values of the inclination of the light-time orbit. The limits quoted are those allowed by the errors given in Tables 7 and 10.

i_3	$\mathcal{M}_3(M_\odot)$	i_3	$\mathcal{M}_3(M_\odot)$	i_3	$\mathcal{M}_3(M_\odot)$
90°	0.773	60°	0.899	30°	1.626
	±10		±12		±21
80°	0.785	50°	1.024	20°	2.493
	±10		±12		±32
70°	0.825	40°	1.236	10°	5.722
	±11		±16		±70

Table 12. Properties of four B-type binaries with masses near 5 $M_\odot$.

Star	Mass	Radius	$\log g$	$\log T_{\rm eff}$	$\log L$	Z	Age (Myr)
DI Her A	5.19 ± 0.11	2.68 ± 0.05	4.30 ± 0.02	4.23 ± 0.02	2.73 ± 0.08	0.02	5
DI Her B	4.53 ± 0.07	2.48 ± 0.05	4.31 ± 0.02	4.18 ± 0.02	2.46 ± 0.08		
V760 Sco A	4.98 ± 0.09	3.01 ± 0.07	4.18 ± 0.02	4.23 ± 0.01	2.82 ± 0.05	0.01	40
V760 Sco B	4.62 ± 0.07	2.64 ± 0.05	4.26 ± 0.02	4.21 ± 0.01	2.63 ± 0.06		
U Oph A	5.27 ± 0.09	3.47 ± 0.02	4.08 ± 0.01	4.22 ± 0.01	2.90 ± 0.07	0.02	40
U Oph B	4.74 ± 0.07	3.11 ± 0.04	4.13 ± 0.01	4.19 ± 0.01	2.71 ± 0.07		
MU Cas A	4.66 ± 0.10	4.19 ± 0.05	3.86 ± 0.01	4.17 ± 0.01	2.87 ± 0.06	0.01	100
MU Cas B	4.58 ± 0.09	3.67 ± 0.43	3.97 ± 0.01	4.18 ± 0.01	2.80 ± 0.06		

at the distance given in Table 10; hence, motion in this orbit could influence the Hipparcos parallax.

6.3. Binary systems similar to U Oph

In the literature, we find another three systems with accurate absolute dimensions and masses of all components within 10% of 5 $M_\odot$: DI Her (Popper 1982), V760 Sco (Andersen et al. 1983), and MU Cas (Lacy et al. 2004). Table 12 summarizes the main properties of the four systems; as indicated by the values of $\log g$ for the primary components, DI Her is the least evolved of the four systems, followed by V760 Sco, U Oph, and MU Cas. Interestingly, DI Her and V760 Sco show apsidal motion as well as U Oph.

Stellar models are required to reproduce all observed properties of both stars in each system for a single age t and chemical composition (primarily the metal abundance parameter, Z). t and Z can, however, be freely chosen with reasonable limits, as no external constraints on them are available.

7. Comparison with stellar evolution models

7.1. Comparisons between models

The most stringent comparison with stellar models is made directly with the observed absolute dimensions, i.e. mass M and radius R (or, equivalently, $\log g$). Effective temperatures, $T_{\rm eff}$, and $\log L$ as derived from R and $T_{\rm eff}$ are important as well, but $T_{\rm eff}$ is derived from reddening-corrected colour indices, using theoretical or empirical calibrations, so $T_{\rm eff}$ and $\log L$ are more model-dependent and less reliable than M and R. Additional indirect evidence on the internal structure of the stars is available for stars in eccentric orbits showing apsidal motion, and from the degree of rotational synchronization and orbital circularization achieved during the derived lifetime of the systems. In all cases, models must be able to match all observed properties of both stars in a system for the same age and chemical composition. We discuss these comparisons in turn below.

For the comparisons with stellar evolution theory, we have considered the recent models by Claret (2004; C-04) and by the Padova group (Girardi et al. 2000, P-99). Both models include core overshooting and OPAL opacities; the new Padova models differ from the earlier series (Bressan et al. 1993; Bertelli et al. 1994; Fagotto et al. 1994a,b; Girardi et al. 1996; P-93) in using an improved equation of state and low-temperature opacities from Alexander & Ferguson (1994). Mass loss at all stages is included in the Claret models; in the Padova models only from the RGB phase on.

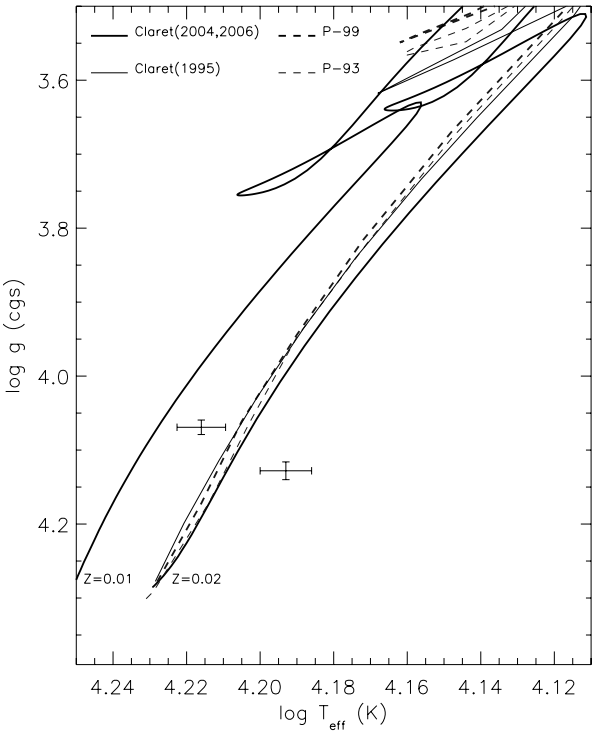

Fig. 7. Evolutionary tracks for 5 $M_\odot$ and $Z = 0.02$ (4 tracks on the right) from C04, P-93, and P-99 in the $\log T_{\rm eff} - \log g$ diagram. The single track on the left is a C-04 model for 5 $M_\odot$ and $Z = 0.01$. The observed observed points for U Oph and their error bars are included for comparison.

As a first step, we compare the models to each other to judge the magnitude of any differences to be verified experimentally. Figure 7 shows the evolutionary tracks through the main-sequence phase for 5 $M_\odot$ and $Z = 0.02$ from C-04, P-93, and P-99 in the $\log T_{\rm eff} - \log g$ diagram. The C-04 model for 5 $M_\odot$ and $Z = 0.01$ and the observed points for U Oph and their error bars are included for comparison. It is immediately clear that any differences between the models for a fixed chemical composition are well within the observational uncertainties; metallicity differences of a factor two (0.3 dex) influence the model predictions far more than subtle differences in the models themselves. Thus, while accurate binary data in principle have the potential to discriminate between different stellar models, they cannot do so in the present case as the metal abundance of our stars is unknown.

We note that the evolutionary speed along the tracks in Fig. 7 might still be different among the models even if the tracks themselves are very similar. However, a precise comparison is difficult, because the models use different conventions to set the zero-point of their age scale (essentially birthline or first equilibrium model). Therefore, isochrones for the same nominal age do not necessarily refer to stars in the same stage of evolution, and we have not pursued this comparison further (see also below).

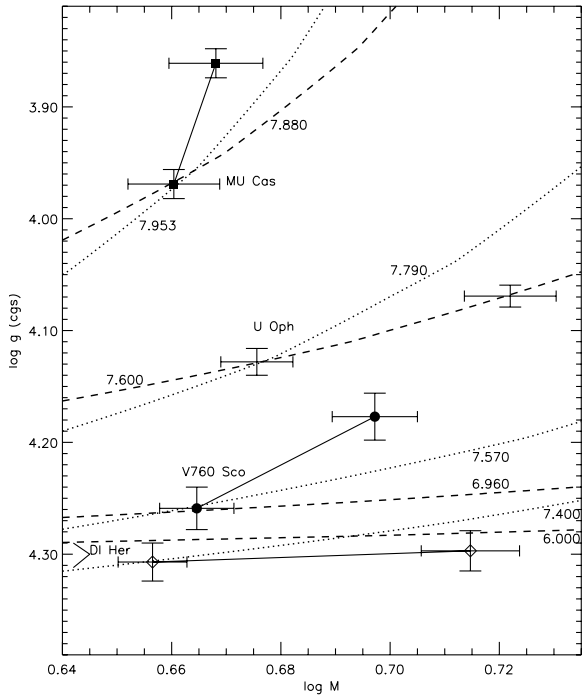

Fig. 8. Observed positions of DI Her, V760 Sco, U Oph, and MU Cas (bottom to top) in the $\log M - \log g$ diagram. C-04 isochrones for $Z = 0.02$ (dashed) and $Z = 0.01$ (dotted) are shown for each system, constrained to pass through the secondary star (not quite possible for DI Her at $Z = 0.02$). log(age) is given for each isochron.

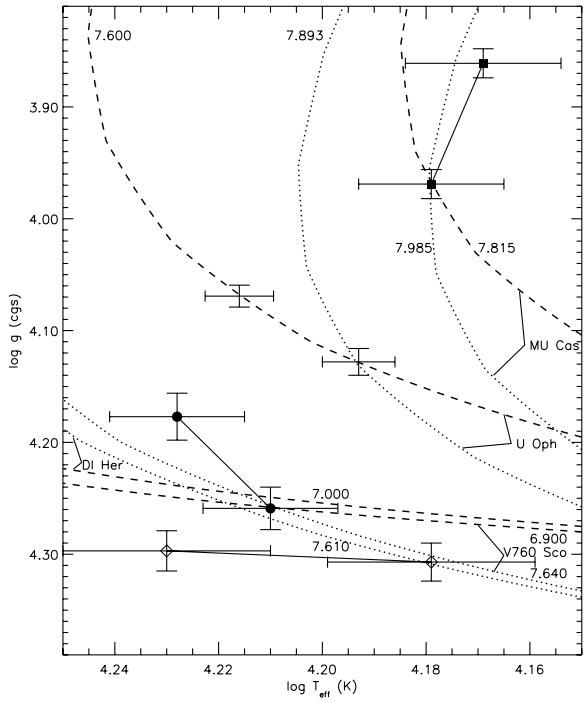

Fig. 9. As Fig. 8, but in the diagram of $\log T_{\rm eff}$ vs. $\log g$.

7.2. Composition differences

Thus, our binary stars provide only weak constraints on the models themselves. However, the degree to which they can be fit with models of a single "Population I" metallicity is of considerable interest in the context of Galactic evolution models, because they provide essentially a snapshot of the chemical diversity of stars formed today (by Galactic standards).

Figures 8 and 9 compare the observed data for all four systems with isochrones from the C-04 models for $Z = 0.02$ and 0.01 in the $\log M - \log g$ and $\log T_{\rm eff} - \log g$ diagrams. Because the less massive star in each system is the least affected by evolution, the four pairs of isochrones have been constrained to match the secondary star in each system precisely (for two different ages for the two values of Z). Unlike for the Sun, we have no external constraint on age or composition for our stars, but for a given Z we can ask if the faster-evolving primary star matches the isochron defined by the secondary. Note that only M and R, but not $\log T_{\rm eff}$ enter in Fig. 8, so an evolutionary track in this diagram is a vertical line if mass loss is negligible; the tracks for 5 $M_\odot$ in Fig. 9 are shown in Fig. 7.

Figures 8 and 9 show that DI Her, V760 Sco, U Oph, and MU Cas cannot all be fit precisely by C-04 models of the same chemical composition: DI Her and U Oph are well matched by models for $Z = 0.02$ (used to fit the Sun in these models), while V760 Sco and MU Cas require models with $Z = 0.01$ or even lower. Thus, there seems to be a range in metallicity of perhaps a factor two in this sample of stars born within the last 100 Myr, an interesting result in view of the ongoing discussion of the (non-)uniqueness of the age-metallicity relation in the Solar neighbourhood (see e.g. Nordström et al. 2004; Haywood 2006; and Holmberg et al. 2006).

We have tested the reliability of this result by asking if a single metallicity could be found for which the models would fit all four systems plausibly rather than precisely. After some exploration, $Z = 0.017$ appeared to be the most promising, and models for the precise mass, M, as well as $M \pm \sigma(M)$ for each of the eight stars were computed for this composition. Isochrone segments were then interpolated so as to best fit each system in the $\log M - \log g$ and $\log T_{\rm eff} - \log g$ diagrams for a single age.

Figures 10 and 11 show that models for $Z = 0.017$ are indeed able to fit DI Her, V760 Sco, U Oph and MU Cas to within $\sim 1.5\sigma$ in $\log M$, $\log g$, and $\log T_{\rm eff}$ for ages of 6.6, 27, 49 and 87 Myr, respectively. Lower-metallicity models are needed to bring $\log g$ for V760 Sco within 1σ of the observed values, while higher metallicities are required for a similarly close match to the temperatures of DI Her and U Oph. The factor two range in Z suggested by Figs. 8 and 9 cannot be claimed with confidence, however. More accurate data for DI Her and V760 Sco are needed to settle the issue, and a programme to obtain them is under way.

7.3. Apsidal motion constants

Three of our systems, DI Her, V760 Sco, and U Oph present apsidal motion. The most evolved of the four systems, MU Cas, shows no evidence of apsidal motion, but the number of cycles observed accurately by Lacy et al. (2004) is too small for any precise determination.

For binary systems with apsidal motion, the ratio between the anomalistic orbital period and the apsidal motion period can be written (Martynov 1973) as:

$$\frac{P_{\rm ano,ecl}}{U} = \sum_{j=2}^{4} \sum_{i=1}^{2} c_{ji} k_{ji} = (22.00 \pm 0.15) \times 10^{-5}, \qquad (3)$$

where k_{ji} are the apsidal motion constants and c_{ji} the coefficients, i (=1, 2) denotes the eclipsing components and j (=2, 3, 4) the order of the coefficients, respectively, and the numerical value corresponds to the case of U Oph. The coefficients c_{ji} decrease strongly with the order j, so we can neglect $j > 2$ as a first approximation.

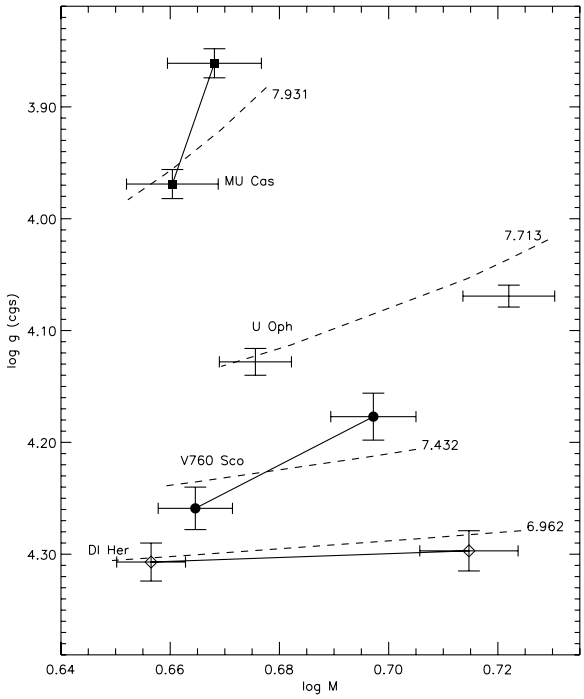

Fig. 10. As Fig. 8, but isochrones for models with $Z = 0.017$.

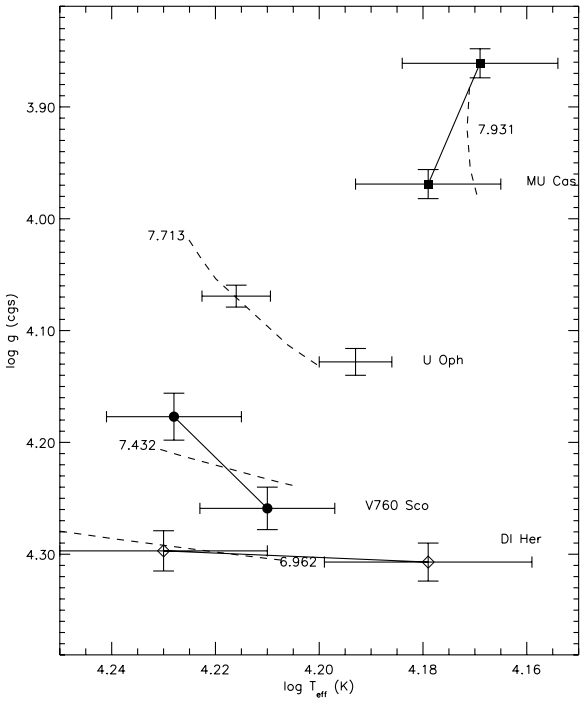

Fig. 11. As Fig. 9, but isochrones for models with $Z = 0.017$.

Before comparing with models, we must correct the observed motion for the relativistic contribution (Levi-Civita 1937; Kopal 1978; major axis A and masses in solar units):

$$\dot{\omega}_{\rm relat} = 0.00229 \frac{m_1 + m_2}{A(1+e^2)} = (1.79 \pm 0.22) \times 10^{-3} \, \frac{\rm degrees}{\rm cycle}, \quad (4)$$

corresponding to a mean value of $\log \bar{k}_{2,\rm obs} = -2.257 \pm 0.055$ for U Oph. Theoretical values of $\log k_2$ have been computed for the C-04 models in the framework of static tides; for dynamical tides, the effects of the compressibility of the stellar fluid (and resonances, if present) should be also considered (Claret & Willems 2002). For both V760 Sco and U Oph, the observed and theoretical values are in good agreement.

DI Her presents a known problem in that already the relativistic term (which corresponds to $U = (5.3 \pm 2.0) \times 10^3$ yr) corresponds to much faster apsidal motion than the observed rate $(34.6 \pm 5.0) \times 10^4$ yr; Guinan et al. 1994), yielding non-physical negative values for the classical term k_2 (Claret 1998). Hence, we do not discuss DI Her any further here, but note that we plan to redetermine the parameters of this system with modern methods to verify the reality of the discrepancy.

7.4. Circularization and synchronization times

In the radiative envelopes of our stars, only radiative damping is relevant in the calculation of the critical times for circularisation of the orbit and and synchronization of the rotation of the components (Claret 2005; Claret & Cunha 1997). For U Oph we find $t_{\rm sync} = 3.6$ Myr (mean for both stars) and $t_{\rm circ} = 67$ Myr, consistent with the observed synchronisation of the stars and slight residual eccentricity of the orbit.

The presence of the tertiary component was not taken into account in these critical age estimations, but it may influence the orbit circularisation time. The triple system V906 Sco (Alencar et al. 1997) is older than its predicted circularisation time; yet, the eclipsing pair shows apsidal motion in an orbit of small eccentricity. According to Mazeh & Shaham 1979) and Mazeh (1990), a third component can introduce slight, periodic modulations of the orbital eccentricity of the close pair, making it possible to find triple systems with eccentric orbits beyond the theoretically predicted circularization time.

8. Conclusions

We have determined the masses and radii of the stars in U Oph with an accuracy of 1–2% from new radial velocities and *uvby* light curves. The ephemeris of the system has also been redetermined, using a modified version of the exact method by Lacy (1992) to analyse 353 times of minimum covering more than 120 years – over 26 700 cycles of the eclipsing pair, almost 6 complete cycles of the apsidal motion, and more than 3 complete orbits of the third component. In the process, we have improved the WD model to treat apsidal motion and light-time orbits at the same time. The improved data also lead to a better determination of the distance to U Oph, the Hipparcos parallax probably being affected by the orbital motion around the third star.

We discuss the new results for U Oph in conjunction with similarly precise data for the systems DI Her (Popper 1982), V760 Sco (Andersen et al. 1983), and MU Cas (Lacy et al. 2004), all with masses within 10% of 5 $M_\odot$. The precise values of $\log g$ for the stars clearly show DI Her, V760 Sco, U Oph, and MU Cas to range from the bottom to the top of the main-sequence band, in order of increasing age (5–100 Myr).

Comparing two recent series of stellar evolution models for the mass of our stars, we find that model differences are well below what can be resolved within the accuracy of our data, and considerably smaller than that caused by a change in Z from 0.02 (solar) to 0.01. Thus, given that our systems all have mass ratios in the range 0.87–0.98 and are all in the main-sequence phase, and that no spectroscopic [Fe/H] value is available, our data cannot rule out any of the currently best stellar evolution models.

Truly critical tests are only possible in systems of known chemical composition and/or large mass ratios and with stars in appreciably different stages of evolution (see Andersen et al. 1991 for a striking example).

We find that different metallicities are needed to fit the four systems, DI Her and U Oph requiring a solar-like $Z = 0.02$ for a precise fit, while V760 Sco and MU Cas are only well matched for a metal abundance of $Z = 0.01$ or even lower. Thus, the chemical evolution of the solar neighbourhood seems to be inhomogeneous even today, with stars of different metallicity having been formed during the last 100 Myr or so – a negligible interval in terms of Galactic chemical evolution or orbital migration. However, given that models for a single metallicity ($Z = 0.017$) still yield a plausible, even if notably poorer fit to the four systems, better data are needed to define the precise range of chemical compositions seen in the sample.

Acknowledgements. We thank Dr. Claud Lacy, who kindly made his ephemeris code available to us. Support for the observations from ESO and the Danish Natural Science Research Council is gratefully acknowledged, as is the financial support of the Brazilian institutions CNPq, CAPES, FAPEMIG and FINEP (to LPRV). This research has made use of the SIMBAD database, operated at CDS, Strasbourg, France, and of NASA's Astrophysical Data System bibliographic services. We thank the referee, Dr. P.F.L. Maxted, for thoughtful comments that led us to improve the paper.

References

Agerer, F., & Hübscher, J. 2003, IBVS, 5484
Alencar, S. H. P., & Vaz, L. P. R. 1997, A&A, 326, 257
Alencar, S. H. P., & Vaz, L. P. R. 1999, A&AS, 135, 555
Alencar, S. H. P., Vaz, L. P. R., & Helt, B. E. 1997, A&A, 326, 709
Alencar, S. H. P., Vaz, L. P. R., & Nordlund, Å. 1999, A&A, 346, 556
Alexander, D. R., & Ferguson, J. W. 1994, ApJ, 437, 879
Andersen, J. 1975a, A&A, 44, 355
Andersen, J. 1975b, A&A, 44, 445
Andersen, J. 1991, A&ARv, 3, 91
Andersen, J., Clausen, J. V., & Nordström, B. 1980, IAU Symp. 88, ed. M. J. Plavec, D. M. Popper, & R.K. Ulrich (Dordrecht: Riedel), 81
Andersen, J., Clausen, J. V., Nordström, B., & Reipurth, B. 1983, A&A, 121, 271
Andersen, J., Clausen, J. V., Nordström, B., & Popper, D. M. 1985, A&A, 151, 329
Andersen, J., Clausen, J. V., Nordström, B., Tomkin, J., & Mayor, M. 1991, A&A, 246, 99
Andersen, J., & Nordström, B. 1983a, A&A, 122, 23
Andersen, J., & Nordström, B. 1983b, A&AS, 53, 287
Batten, A. H., & Scarfe, C. D. 1977, Rev. Mex. Astron. Astrofis., 3, 21
Bressan, A., Fagotto, F., Bertelli, G., & Chiosi, C. 1993, A&AS, 100, 647
Bertelli, G., Bressan, A., Chiosi, C., Fagotto, F., & Nasi, E. 1994, A&AS, 106, 275
Bozkurt, Z., & Değirmenci, Ö. L. 2005, in The Light-Time Effect in Astrophysics, ed. C. Sterken, ASP Conf. Ser., 335, 277
Bruch, A. 1999, AJ, 117, 3031
Casey, B. W., Mathieu, R. D., Vaz, L. P. R., Andersen, J., & Suntzeff, N. B. 1998, AJ, 115, 1617
Cester, B., Fedel, B., Giuricin, G., Mardirossian, F., & Mezzetti, M. 1978, A&AS, 33, 91
Claret, A. 1995, A&AS, 109, 441
Claret, A. 1997, A&AS, 125, 439
Claret, A. 1998, A&A, 330, 533
Claret, A. 2000, A&A, 359, 289
Claret, A. 2004, A&A, 424, 919
Claret, A. 2005, in Tidal Evolution and Oscillations in Binary Stars: Third Granada Workshop on Stellar Structure, ed. A. Claret, A. Giménez, & J.-P. Zahn, ASP Conf. Ser., 333, 116
Claret, A., & Cunha, N. C. S. 1997, A&A, 318, 187
Claret, A., & Giménez, A. 1998, A&AS, 133, 123
Claret, A., & Willems, B. 2002, A&AS, 388, 518
Crawford, D. L. 1974, Dudley Obs. Rep., 9, 17
Crawford, D. L. 1975, PASP, 87, 481
Crawford, D. L. 1978, AJ, 83, 48
Crawford, D. L. 1979, Dudley Obs. Rep., 14, 23
Davis, J., & Shobbrook, R. R. 1977, MNRAS, 178, 651
Diethelm, R. 2004, IBVS, 5543
Eaton, J. A., & Ward, D. H. 1973, ApJ, 185, 921
Eddington, A. S. 1926, MNRAS, 178, 651
Eritsian, M. A., Docobo, J. A., Melikian, N. D., & Tamazian, V. S. 1998, A&A, 329, 1075
Fagotto, F., Bressan, A., Bertelli, G., & Chiosi, C. 1994a, A&AS, 104, 365
Fagotto, F., Bressan, A., Bertelli, G., & Chiosi, C. 1994b, A&AS, 105, 29
Giménez, A., & Garcia-Pelayo, J. M. 1983, Ap&SS, 92, 203
Giménez, A., & Clausen, J. V. 1986, A&A, 161, 275
Giménez, A., & Bastero, M. 1995, Ap&SS, 226, 99
Giménez, A., Clausen, J. V., & Andersen, A. 1986, A&A, 160, 310
Girardi, L., Bressan, A., Chiosi, C., & Bertelli, G., Nasi, E. 1996, A&AS, 117, 113
Girardi, L., Bressan, A., Bertelli, G., & Chiosi, C. 2000, A&AS 141, 371
Guinan, E. F., Marshal, J. J., & Maloney, F. P. 1994, IBVS, 4101
Haywood, M. 2006, MNRAS 371, 1760
Holmberg, J., Nordström, B., & Andersen, J. 2006, A&A, submitted
Holmgren, D. E., Hill, G., & Fisher, W. 1991, A&A, 248, 129
Irwin, J. B. 1952, ApJ, 116, 211
Irwin, J. B. 1959, AJ, 64, 149
Kallrath, J., & Linnell, A. P. 1987, ApJ, 313, 346
Kazarovets, A. V., Samus, N. N., Durlevich, O. V., Frolov, M. S., & Antipin, S. V. 1999, IBVS, 4659
Klimec, Z. 1972, IBVS, 637
Koch, R. H., & Koegler, C. A. 1977, ApJ, 214, 423
Koch, R. H., Olson, E. C., & Yoss, K. M. 1965, ApJ, 141, 955
Kopal, Z. 1968, Ap&SS, 2, 166
Kopal, Z. 1978, Dynamics of Close Binary Systems (Dordrecht, Holland: Reidel)
Kurucz, R. L. 1979, ApJS, 40, 1
Kwee, K. K., & Van Woerden, H. 1956, Bull. Astron. Inst. Neth., 12, 327
Kämper, B.-C. 1986, Ap&SS, 120, 167
Lacy, C. H. S. 1992, AJ, 104, 2213
Lacy, C. H. S., Claret, A., & Sabby, J. A. 2004, AJ, 128, 1840
Levi-Civita, T. 1937, Amer. J. Math., 59, 225
Martynov, D. Ya. 1973, in Eclipsing Variable Stars, ed. V. P. Tsesevich, IPST Astrophys. Library, Jerusalem, 291
Mazeh, T. 1990, AJ, 99, 675
Mazeh, T., & Shaham, J. 1979, A&A, 77, 145
Milne, E. A. 1927, MNRAS, 87, 43
Moffat, A. F. J., Vogt, N., Vaz, L. P. R., & Grønbech, B. 1983, A&A, 120, 278
Napiwotzki, R., Schönberner, D., & Wenske, V. 1993, A&A, 268, 653
Nielsen, R. F., Nørregaard, P., & Olsen, E. H. 1987, ESO Messenger, 50, 45
Nordlund, Å., & Vaz, L. P. R. 1990, A&A, 228, 231
Nordström, B., Mayor, M., Andersen, J., et al. 2004, A&A, 418, 989
Olsen, E. H. 1983, A&AS, 54, 55
Panchatsaram, T. 1981, Bull. Astr. Soc. India, 9, 139
Plavec, M., Pěkný, Z., & Zmatanová, M. 1960, Bull. Astr. Inst. Czech., 11, 180
Press, W. H., Flannery, B. P., Teukolsky, S. A., & Vetterling, W. T. 2000, Numerical Recipes (New Delhi, India: Cambridge University Press), 678
Popovici, C. 1971, IBVS, 508
Popper, D. M. 1980, ARA&A, 18, 115
Popper, D. M. 1981, ApJS, 47, 339
Popper, D. M. 1982, ApJ, 254, 203
Popper, D. M., & Carlos, R. 1970, PASP, 82, 762
Slettebak, A., Collins II, G. W., Boyer, P. B., White, N. M., & Parkinson, T. D. 1975, ApJS, 29, 137
Shobbrook, R. R. 1976, MNRAS, 176, 673
Van Hamme, W. 1993, AJ, 106, 2096
Vaz, L. P. R. 1984, Ph.D. Thesis, Copenhagen Univ. Obs.
Vaz, L. P. R. 1985, Ap&SS, 113, 349
Vaz, L. P. R. 1985, Rev. Mex. Astron. Astrophys., 12, 177
Vaz, L. P. R., & Nordlund, Å. 1985, A&A, 147, 281
Vaz, L. P. R., Andersen, J., & Rabello Soares, M. C. A. 1995, A&A, 301, 693
Vaz, L. P. R., Cunha, N. C. S., Vieira, E. F., & Myrrha, M. L. M. 1997, A&A, 327, 1094
Vaz, L. P. R., Andersen, J., Casey, B. W., et al. 1998, A&AS, 130, 245
Vieira, L. A. 2003, MSc Dissertation, Federal University of Minas Gerais
von Zeipel, H. 1924, MNRAS, 84, 665
Wilson, R. E. 1979, ApJ, 234, 1054
Wilson, R. E. 1993, in New Frontiers in Binary Star Research, ed. K. C. Leung, & I.-S. Nha, ASP Conf. Ser., 38, 91
Wilson, R. E., Devinney, E. J. 1971, ApJ, 166, 605
Wolf, M., Harmanec, P., Diethelm, R., Hornoch, K., & Eenens, P. 2002, A&A, 383, 533
Zejda, M. 2004, IBVS, 5583